Airborne lidar study of the vertical distribution of aerosols over Hyderabad, an urban site in central India, and its implication for radiative forcing calculations

H. Gadhavi, A. Jayaraman

Ann. Geophys., 24, 2461–2470, 2006
www.ann-geophys.net/24/2461/2006/

Annales Geophysicae

Airborne lidar study of the vertical distribution of aerosols over Hyderabad, an urban site in central India, and its implication for radiative forcing calculations

H. Gadhavi and A. Jayaraman

Physical Research Laboratory, Ahmedabad 380 009, India

Received: 13 March 2006 – Revised: 25 July 2006 – Accepted: 24 August 2006 – Published: 20 October 2006

Abstract. Use of a compact, low power commercial lidar onboard a small aircraft for aerosol studies is demonstrated. A Micro Pulse Lidar fitted upside down in a Beech Superking aircraft is used to measure the vertical distribution of aerosols in and around Hyderabad, an urban location in the central India. Two sorties were made, one on 17 February 2004 evening hours and the other on 18 February 2004 morning hours for a total flight duration of four hours. Three different algorithms, proposed by Klett (1985), Stephens et al. (2001) and Palm et al. (2002) for deriving the aerosol extinction coefficient profile from lidar data are studied and is shown that the results obtained from the three methods compare within 2%. The result obtained from the airborne lidar is shown more useful to study the aerosol distribution in the free troposphere than that obtained by using the same lidar from ground. Using standard radiative transfer model the aerosol radiative forcing is calculated and is shown that knowledge on the vertical distribution of aerosols is very important to get more realistic values than using model vertical profiles of aerosols. We show that for the same aerosol optical depth, single scattering albedo and asymmetry parameter but for different vertical profiles of aerosol extinction the computed forcing values differ with increasing altitude and improper selection of the vertical profile can even flip the sign of the forcing at tropopause level.

Keywords. Atmospheric composition and structure (Aerosols and particles; Instruments and techniques) – Meteorology and atmospheric dynamics (Radiative processes)

1 Introduction

Aerosols play a major role in determining the regional scale radiation budget of the earth's atmosphere by directly scattering and absorbing the incoming and outgoing radiations as well as through modifying cloud properties, such as the cloud droplet size distribution and cloud lifetime (e.g. Twomey, 1974; Albrecht, 1989; Pincus and Baker, 1994; Haywood and Boucher, 2000; Kaufman et al., 2005; Ramanathan el al., 2005). Nevertheless, measurements of aerosol properties, particularly their vertical distribution are less and unevenly distributed around the globe. Over India, knowledge on the vertical distribution of aerosols has come mostly from in situ probing using rocket and balloon-borne instrumentations (Jayaraman et al., 1987; Jayaraman and Subbaraya, 1993; Ramachandran and Jayaraman, 2003), ground-based lidar measurements (Devara et al., 1995; Jayaraman et al., 1995; Parameswaran et al., 1998) as well as from remote-sensing satellites (Kent et al., 1998; Spinhirne et al., 2005). Airborne lidars are gaining popularity in recent years as they provide useful information on the aerosol vertical profiles over a wider region such as during the INDOEX (Pelon et al., 2002), SAFARI-2000 (McGill et al., 2003), ACE-2 (Flamant et al., 2000) etc. Airborne laser remote sensing has additional advantage that it can measure aerosol profiles both in vertical as well as horizontal directions in very short time and can be a good tool to quantify the aerosol properties in the three-dimensional space.

Under the Indian Space Research Organization's (ISRO) Geosphere Biosphere Programme (GBP) a land campaign was conducted in the central India during February 2004 (to be referred henceforth as LC-1) to study the aerosol properties and different trace gases concentrations. During LC-1, for the first time in India, airborne lidar measurements were carried out over Hyderabad, one of the major industrialized cities located in the central India. Results obtained from this airborne lidar experiment are discussed in the present paper in the context of their implication to radiative forcing calculations. Section 2 of the paper describes instrumentation and data reduction while Sect. 3 describes retrieval of aerosol extinction profile and highlights the difference between three

Correspondence to: H. Gadhavi
(harish.gadhavi@gmail.com)

Published by Copernicus GmbH on behalf of the European Geosciences Union.

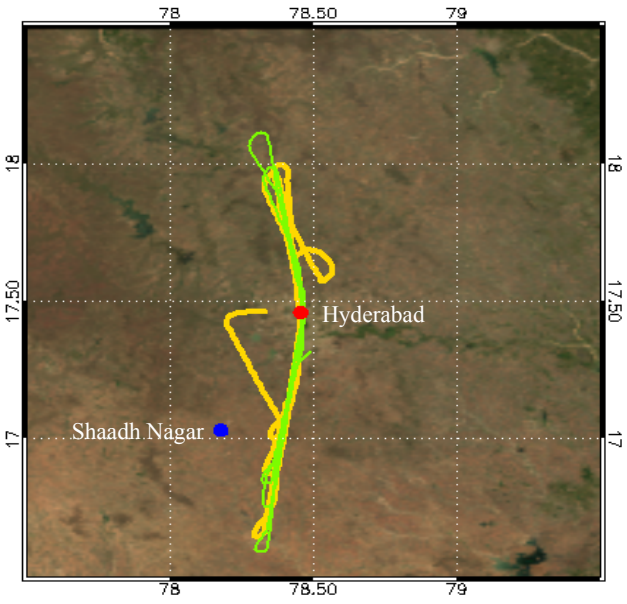

Fig. 1. Ground track of the airborne lidar measurements made on 17 February 2004 (Yellow line) and 18 February 2004 (Green line). The background image is created from MODIS surface reflectance data for the visible wavelength region.

major retrieval algorithms. In Sect. 4 discussions on observed aerosol properties and their implications to aerosol radiative forcing are presented. In Sect. 5, major conclusions from this first Indian airborne lidar experiment are presented.

2 Instrumentation and data reduction

The Micro Pulse Lidar (MPL) which was originally developed by NASA (Spinhirne, 1993) and later made available commercially is used in the present airborne study. It is a monostatic co-axial system with 20 cm diameter Schmidt-Cassegrain telescope and employs a diode pumped Nd-YLF laser giving out pulsed laser output in second harmonics at 523.5 nm wavelength. The pulse repetition rate is configured at 2500 Hz. The lidar has the specification of obtaining the vertical profiles of aerosols from ground level up to about 30 km altitude with a range resolution of 30 m. The National Remote Sensing Agency at Hyderabad provided the aircraft (Raytheon Aircraft, Beech Super King Air 200 series) for this purpose. MPL was mounted in the aircraft looking downward through a window originally available at the belly of the aircraft for aerial photography purpose. To avoid direct reflectance from the glass window coming back into the telescope, the lidar mount was kept tilted at 6° with respect to the normal of the window glass pan. This 6° tilt results in an over estimation of the atmospheric height by about 44 m at the maximum aircraft altitude of 8 km and by about 11 m for the boundary layer top height of ∼2 km. No special correction is applied for the inclination, while discussing the results on the vertical distribution of aerosols. Measured backscattered signal strength data are summed for 15 s, which corresponds to a total of 37 500 profiles and averaged before storing as a single profile. This results into 1.3 km resolution in the horizontal direction for the typical aircraft speed of 320 km/h. A total of two sorties were made, one on 17 February 2004 evening between 18:40 to 20:40 h (local standard time) and another on 18 February 2004 morning between 08:50 to 10:50 h. Figure 1 shows the ground track of the sorties made in these two days. Sorties were made mainly in the north-south direction to facilitate measurements perpendicular to the wind direction, which is mainly easterly over Hyderabad during February. About 450 profiles were obtained on each day.

Aerosol extinction profile from the measured backscatter intensity is retrieved in two steps. First, the normalized relative backscatter (NRB) profile is obtained by correcting for afterpulse effect, overlap correction, energy normalization, range correction etc. as described in Campbell et al. (2002) and Gadhavi (2005). The second step is to calculate extinction profile from NRB, which is described in Sect. 3. The overlap correction factor was obtained by making lidar measurements in the horizontal direction from Mt. Abu at the Gurushikhar observatory (24.65° N, 72.78° E) of Physical Research Laboratory. NRB profiles can be described mathematically as,

$$\frac{z^2\{P(z) - p_{ap}(z) - p_b\}}{O(z)E} = C\ \left(\beta_m(z) + \beta_p(z)\right)\ T^2(z) \quad \text{(1a)}$$

$$T(z) = \exp\left[-\int_0^z \left(\alpha_p(z') + \alpha_m(z')\right) dz'\right] \quad \text{(1b)}$$

where z is the range from the MPL to the target, $P(z)$ is the uncorrected backscattered lidar signal, p_{ap} is the contribution from afterpulse effect, p_b is background contribution, $O(z)$ is overlap correction factor and E is the energy of the transmitted laser pulse. On the right hand side of the equation, C is a constant, also known as calibration constant, β_m and β_p are backscattering coefficients due to air molecules and aerosols respectively, and T is the atmospheric transmission between the MPL receiver and the scattering volume. In Eq. (1b), α_m and α_p are extinction coefficients due to air molecules and aerosols, respectively.

Left hand side of Eq. (1a) is called NRB. At a given altitude NRB values are roughly proportional to aerosol amount present at that altitude. However, due to two way transmission loss the same NRB values at different altitudes represent different aerosol amount. In case of aircraft measurement a given NRB value represents higher aerosol concentration at lower altitude and vice versa. Figure 2 shows a 2-D colour map of the NRB values obtained on 17 and 18 February 2004. Distinct marking of the boundary layer top is seen on both the days around 2 km above ground level. Also

on 17th when observations were made during sun-set hours a gradual decrease in the aerosol amount is seen within the boundary layer with time. As the surface cools, thermal eddies decrease, which otherwise help in lifting particles from surface layer to higher heights. On 18th when measurements were made during morning hours, an increase in the boundary layer aerosol amount is seen when eddy mixing increases with increasing surface and air temperatures.

3 Aerosol extinction profile

NRB profiles are averaged to get a single profile for each sortie, while data obtained during aircraft ascent, descent and when the aircraft takes curves are omitted.

Retrieval of extinction profile from NRB involves few important assumptions. These assumptions are a priori knowledge of extinction-to-backscatter ratio and extinction (or backscattering) coefficient at a reference range. Accuracy of retrieved quantity critically depends on these assumptions and algorithms are developed to minimize the effects of the assumptions on the final output. Klett (1981, 1985) describe methods in which it is suggested for the first time that reference range to be specified at far end of lidar observation-range in order to make algorithm stable and less sensitive to errors in reference extinction (or backscattering) value. It is also shown using simulation that even if two algorithms are mathematically equal, they can perform quite differently for different numerical methods. Assumptions made for one situation are quite often not applicable to other situation. Ground-based lidar observations in vertical direction has free troposphere or stratosphere in the far-end, where aerosol concentration is low and less variable than at boundary layer, which is the far-end for airborne observations.

Relatively few literature exists to describe algorithms for airborne or space borne lidar measurements. We took this as an opportunity to review three algorithms for their ease of implementation, stability in numerical performance and sensitivity to assumptions. The three algorithms reviewed are transmittance solution described by Palm et al. (2002), optimum estimation method described by Stephens et al. (2001) and Klett (1985) algorithm in forward direction. Henceforth, these algorithms will be referred as P2002, S2001 and K1985, respectively.

P2002 is an operational algorithm for Geoscience Laser Altimeter System (GLAS). GLAS is a space-borne atmospheric lidar and surface altimeter system onboard Ice Cloud and land Elevation Satellite (ICE-Sat) launched in January 2003 by USA (Spinhirne et al., 2005). Unlike most of the algorithms, which involve taking logarithm of NRB, P2002 does not contain logarithmic terms. This is particularly important on occasions when lidar signals could be negative due to random noise. P2002 algorithm will remain stable in such noisy condition. P2002 equation for aerosol backscattering

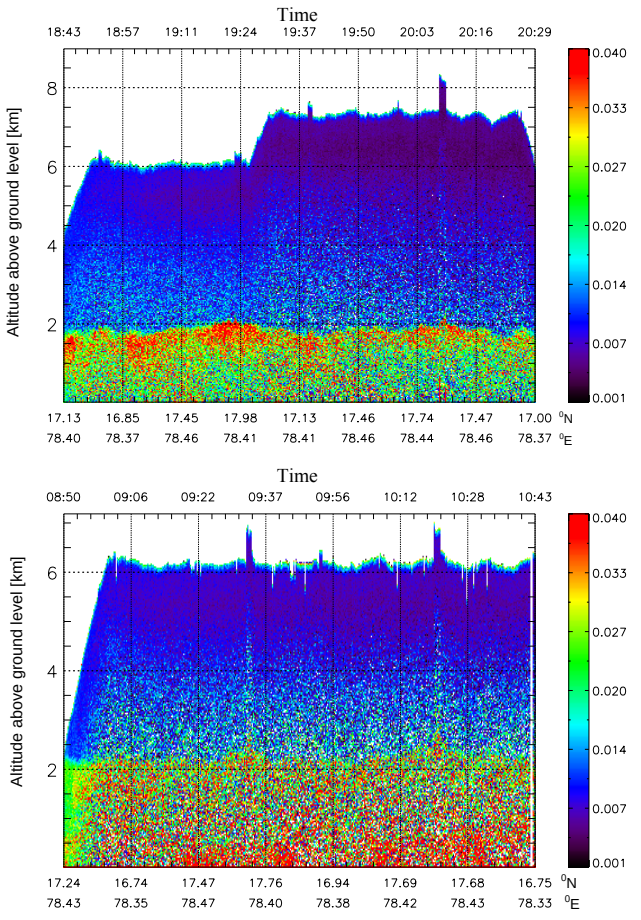

Fig. 2. Normalized Relative Backscatter values in arbitrary unit (proportional to range corrected photons) obtained from the airborne lidar measurements made on **(a)** 17 February 2004 and **(b)** 18 February 2004 over Hyderabad. Latitude and longitude of the ground track are according to measurement sequence. Altitude in km is from ground level, which is about 530 m above the mean sea level. For both the days boundary layer top is seen around 2 km but aerosol distribution within the boundary layer is quite different.

coefficient $\beta_p(z)$, assuming single scattering event and for nadir measurement is shown below:

$$\beta_p(z) = \frac{T_m^{2(X-1)}(z)P'(z)}{I(z_t) - 2L_p \int_{z_t}^{z} T_m^{2(X-1)}(z')P'(z')dz'} - \beta_m(z) \quad (2a)$$

$$\alpha_p(z) = L_p \beta_p(z) \quad (2b)$$

where, T_m is the transmission due to molecular scattering, β_m is the backscattering coefficient of the air molecules, $P'(z)$ is NRB/C (refer Eq. 1), L_p is an extinction-to-backscattering ratio of aerosol (also known as lidar ratio), X is L_p/L_m and L_m is the extinction-to-backscattering ratio for air molecules. The term $I(z_t)$ in the denominator is two way transmission between telescope and the first bin

from where backscattering coefficients calculations are to be made. When this distance is very small, as in the present case it will be very close to 1. In Eq. (2a), L_m is a known quantity which is equal to $8\pi/3$. Molecular transmission T_m can be calculated fairly accurate from temperature and pressure profiles. U.S. standard atmospheric temperature and pressure profiles (McClatchey et al., 1972) are scaled to the observed surface level pressure and are used in the present case to calculate T_m. Aerosol extinction coefficient (α_p) can be obtained from β_p by multiplying it with L_p as shown in Eq. (2b).

The S2001 algorithm is based on the optimum estimation method, which is quite popular among satellite remote sensing community for retrieval of atmospheric temperature and composition from thermal radiation measurements (Rodger, 1976, 1990, 2000). In this algorithm NRB profile is first constructed by lidar equation using climatological or crude estimate of extinction values and the difference between observed and reconstructed NRB profile is minimized using an iteration loop of the form shown in Eq. (3). This algorithm is mathematically vigorous and demands quite a high computer-memory and processing time in comparison to other two algorithms. However, the very unique and important advantage is that it retrieves simultaneously error estimates of final result for various uncertainties in the input values. A general equation for the optimum estimation algorithm can be written as,

$$\hat{\boldsymbol{x}}^{n+1} = \mathbf{S}_x^n(\mathbf{S}_a^{-1}\boldsymbol{x}_a + \mathbf{K}^{nT}\mathbf{S}_y^{-1}[\boldsymbol{y} - \boldsymbol{f} + \mathbf{K}^n\hat{\boldsymbol{x}}^n]) \tag{3}$$

where $\boldsymbol{x}$ is the resultant vector, the quantity to be retrieved and in the present case the extinction values at different altitudes. $\boldsymbol{y}$ is the measurement vector and in the present case it is a range corrected signal strength and aerosol optical depth. **f** is known as the forward function which relates the measurements to retrievable quantity, which essentially is a lidar equation. $\boldsymbol{S}_x^n$ is an error co-variance matrix for nth iteration. $\mathbf{S}_a$ and $\mathbf{S}_y$ are error co-variance matrices for a priori knowledge of aerosol extinction and measurement errors. **K** is the sensitivity matrix. Superscript T denotes transpose of a matrix and n denotes number of iteration. Symbols in Eq. (3) are kept same as in S2001. More complete explanation of the symbols is available in Stephens et al. (2001).

Klett (1981) presents two solutions, one refers to solving the lidar equation with reference value provided at near end while other refers to solving lidar equation with reference value provided at far end. Solution presented in Klett (1981) is further elaborated for separating Rayleigh contribution and range dependent lidar ratio in K1985. It should be noted that focus of Klett (1981) is to show better stability of far-end solution in comparison to near-end solution. K1985 solution with near end reference value is not much different than previously existing lidar solutions such as Fernald et al. (1972). Following are equations for near end solution based on Klett's (1985) solution for backscattering coefficient assuming a constant lidar ratio.

$$\beta(r) = \frac{\exp(S' - S'_0)}{\left[\beta_0^{-1} - 2L_p \int_{r_0}^{r} \exp(S' - S'_0)dr'\right]} \tag{4a}$$

$$S' - S'_0 = S - S_0 + 2L_m \int_{r_0}^{r} \beta_m dr' - 2L_p \int_{r_0}^{r} \beta_m dr' \tag{4b}$$

$$S(r) = \log(\mathrm{NRB}(r)) \tag{4c}$$

where, β is the total backscattering by air molecules and aerosols. Subscript m denotes molecular scattering and p denotes particulate (aerosol) scattering. L is the lidar ratio as explained in Eq. (2). Subscript 0 denotes the reference range near lidar telescope.

Poor stability in near end solution for ground based vertical observation of lidar is due to the denominator term in Eq. (4a). It decreases rapidly with increasing range because of reduction in aerosol concentration and air density, which makes solution numerically unstable. However in case of airborne or space-borne lidar observation aerosol concentration and air density increases with range and hence near-end solution is expected to be stable than compared to ground-based observation. Also for airborne observations reference range at far-end can not be guessed as reasonably as in the case of ground based observations and hence near-end solution becomes a good choice for the airborne observations.

Calibration constant "C" and lidar-ratio L_p are prerequisite to compute extinction coefficient as evident from Eqs. (1) to (4). The calibration constant "C" can be calculated by knowing extinction (or backscattering) coefficient at reference range. In case of high altitude airborne or space-borne measurements it can be obtained by comparing the NRB profile with modelled Rayleigh backscattering profile for air molecules in the stratosphere. But in the free tropical troposphere significant amount of aerosol could be present. Ramachandran and Jayaraman (2003) have reported a value of $0.02\,\mathrm{km}^{-1}$ for aerosol extinction at the altitude of 5.5 km using balloon borne sun-photometer over Hyderabad in April 2001. However, Hart et al. (2005) report aerosol extinction over the Indian Ocean region close to zero above 3 km using GLAS observation. In the absence of independent measurements of aerosol extinction or backscattering coefficient during our experiment, we have carried out sensitivity analysis for reference values used to estimate "C". Aerosol backscattering coefficient at reference range is varied between 0 and $6\times10^{-4}\,\mathrm{km}^{-1}\,\mathrm{sr}^{-1}$ so as to cover observed extinction value for a wide range of lidar-ratios. Results of this sensitivity analysis are discussed in the next few paragraphs.

A priori knowledge of lidar-ratio is necessary to derive the extinction profile apart from knowing the backscattering coefficient value at the reference range. In the present

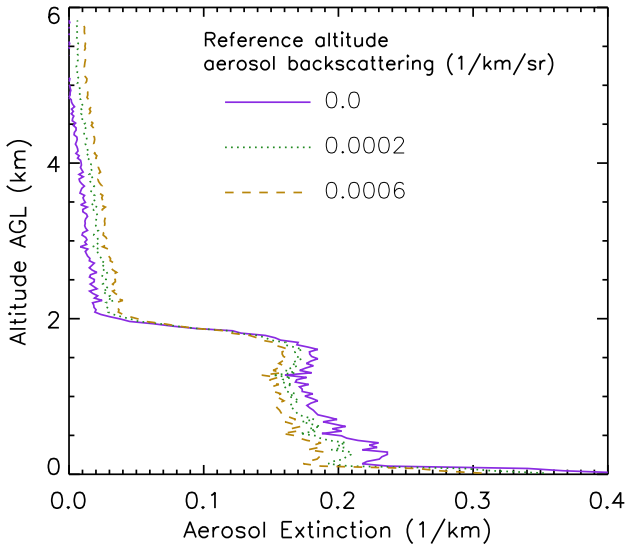

Fig. 3. Sensitivity of aerosol extinction profile retrieved by algorithm described in Palm et al. (2002) to assumed values of aerosol backscattering coefficient at a reference altitude of 6 km.

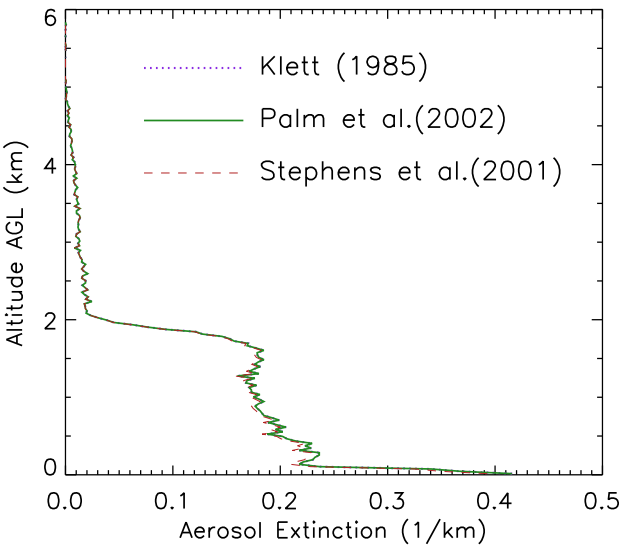

Fig. 4. Comparison of the performance of three algorithms described in Palm et al. (2002), Stephens et al. (2001) and Klett (1985) used for the retrieval of aerosol extinction coefficient profiles from the airborne lidar measurements.

case, the lidar-ratio is obtained by an iterative process in which independently measured column AOD values using sun-photometer are employed to constrain the extinction values and the constrain is applied by adjusting the lidar-ratio. Ideally an extinction profile should be available up to top of the atmosphere in order to compare it with the column AOD. During volcanically quiescent period there is very less aerosol amount present at higher altitudes; for example AOD above 6 km measured by SAGE-II on 28 February 2004 over 19.3° N Latitude and 80.6° E Longitude is 0.015±0.004. Column AOD observations made from a nearby station (Shaadh Nagar, Fig. 1) are found to be 0.4±0.05 on 17 February and 0.29±0.01 on 18 February during periods close to aircraft sorties. In the present case the higher altitude aerosols are found to contribute only about 3 to 5% to the total column AOD, which will result in 2 to 3% error in extinction values. However, lidar-ratio obtained by constraining the extinction profile with AOD is sensitive to assumed value of backscattering coefficient at reference range. For example, in case of "No Aerosol" above 6 km (i.e., β_p=0 for altitude above 6 km) we get a lidar ratio of 45.2 sr, whereas for β_p=6×10^{-4} km^{-1} sr^{-1} at 6 km, the lidar-ratio is 18.9 sr. Aerosol extinction profiles for three different values of reference aerosol backscattering coefficient (viz., β_p=0; 2×10^{-4} km^{-1} sr^{-1} and 6×10^{-4} km^{-1} sr^{-1} at altitude around 6 km) using the P2002 algorithm are shown in Fig. 3. When retrieval of extinction profile is constrained with AOD, the effect is to shift the extinction profile in one direction in free troposphere and in the opposite direction in boundary layer (Fig. 3). A 50% uncertainty in the total (Air molecules + Aerosols) backscattering coefficient at reference range leads to approximately an error of 20% in the derived aerosol extinction coefficient at lower altitudes. S2001 and K1985 algorithms have similar sensitivity to the assumed backscattering coefficient values at the reference range.

Figure 4 shows the comparison between the results obtained using the three algorithms for 17 February data and assuming zero aerosol-backscattering at reference range. Lidar-ratios for P2002 and K1985 obtained from AOD measurements as explained earlier compare better than one decimal place and so is the extinction profiles. S2001 algorithm has in-built constraint based on AOD and doesn't require to supply lidar-ratio explicitly. Results from these algorithms compare within about 2% and no appreciable bias with altitude is observed in any particular algorithm.

The aerosol extinction profiles obtained from the airborne lidar measurements are compared with that obtained from the ground based observations made using the same lidar from Shaadh Nagar, located around 60 km south of Hyderabad (see Fig. 1 for the location). The ground-based observations are made between 19:30 to 20:30 h on 18 February 2004. Same instrument settings are used in the ground based observation except that photon counts are summed for one minute instead of 15 s as in the case of airborne observations. Kaestner (1986) algorithm is used to retrieve extinction profile for the ground-based measurements, which is similar to Klett's (1985) algorithm but defines the solution directly in terms of extinction coefficient. The aerosol extinction profile is derived by assuming zero aerosol content at far end (about 6 km in the present case). Since ground-based observations were made after sun-set, AOD data are not available for constraining extinction in order to get the lidar-ratio. Hence,

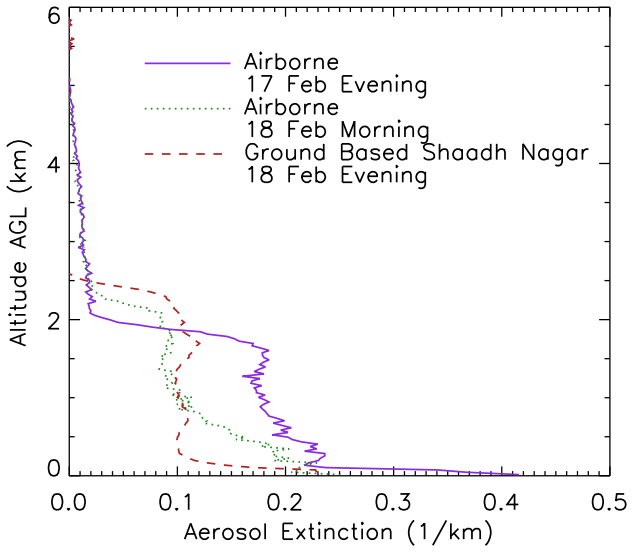

Fig. 5. Comparison of the average aerosol extinction coefficient profiles obtained from airborne lidar measurements made on 17 and 18 Feb with that from ground based measurements made on 18 evening at a nearby location using the same lidar instrument.

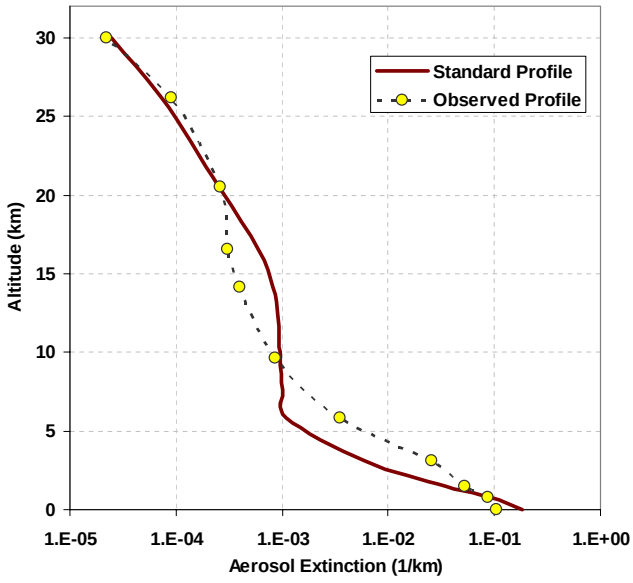

Fig. 6. Aerosol extinction profile with circle and dashed line is obtained by combining air-borne lidar measurements on 17 February and SAGE data at altitudes above 6 km. Extinction profile with solid line is the "standard" model aerosols profile. Comparison of aerosol radiative forcing values computed using these two profiles is shown in Fig. 7.

extinction profile for ground-based observation is retrieved using lidar-ratio equal to 40 sr, which is in between the lidar ratios obtained for airborne measurements made on the two days. Figure 5 shows the ground-based observations along side airborne observations of extinction profiles on 17 and 18 February. Ground-based observations detect almost no aerosol above the boundary layer whereas significant aerosol extinction is seen in the free troposphere from airborne observations on both days. Though the ground-based observation is temporally and spatially separated from the airborne measurements, detection of no aerosol in the free troposphere from ground observations is due to poor signal-to-noise ratio for the data obtained from free tropospheric altitudes. Particularly over polluted urban locations, as in the present case, it is difficult to study aerosols from ground based lidar of moderate power, because of the weak backscattered signal from higher altitudes which is further attenuated by high amount of aerosols found within the boundary layer. From signal-to-noise ratio (S/N) point of view, airborne lidar is found more favourable than the ground based measurements for the free tropospheric aerosol study, particularly over polluted urban locations.

4 Aerosol Radiative Forcing

The measured aerosol extinction profiles are used to calculate the aerosol radiative forcing (ARF), a parameter widely used by modellers for the estimation of the role of aerosols in inducing regional and global scale climate modifications. Radiative forcing is defined as difference in net radiative fluxes at given altitude between aerosol laden atmosphere and aerosol free atmosphere. Though this definition differs with conventional definition of radiative forcing given in IPCC (2001) which defines aerosol radiative forcing for anthropogenic aerosol, it serves the purpose of estimating influence of aerosols (natural + anthropogenic) in radiation budget (Ramanathan et al., 2001). Atmospheric absorption due to aerosols for a given layer is defined as difference between aerosol radiative forcing at top and bottom of the layer. For the sake of brevity, henceforth atmospheric absorption due to aerosol will be mentioned as atmospheric absorption only. The objective of computing ARF in the present study is to examine the sensitivity of the ARF computation to the aerosol vertical distribution. Calculations are carried out using Santa Barbara Discrete ordinate Atmospheric Radiative Transfer (SBDART) model developed by Ricchiazzi et al. (1998). Accuracy of SBDART is better than 3% in shortwave range. SBDART computes radiative fluxes assuming plane parallel atmosphere. Scattered fluxes are estimated using discrete ordinate method (Stamnes et al., 1988) and molecular absorption using LOWTRAN-7 atmospheric transmission band model.

The different input parameters used in the ARF calculations are summarized in Table 1. Aerosol extinction profile from ground to 40 km is constructed by combining the measured profiles from the airborne lidar observations for the lower altitudes (0–6 km) and the smoothed extinction profile from SAGE-II (Ackerman et al., 1989) available for 28

Table 1. Summary of various parameters used in the aerosol radiative forcing calculations.

Class	Parameter	Typical value	Description
Aerosol	Vertical profile	Observed and standard extinction profiles	Observed aerosol extinction profile is constructed from airborne lidar and SAGE-II data, where as standard extinction profile is based on visibility data.
	AOD	0.32	Observed using sun-photometer on 17 Feb 2004, at 500 nm, and average for the day. Spectral dependence is based on model described in Sect. 5
	Single scattering albedo	0.85	At 500 nm for Continental Average aerosol model. In calculations, spectrally varying values for various models are used
	Asymmetry parameter	0.63	
Atmosphere	Temperature and pressure profile	FNL data	(Stunder, 1997)
	Ozone	245 DU	TOMS data
	Water vapour	0.56 cm	Columnar precipitable water vapour measured using MICROTOPS-II Sun-Photometer
Other	Wavelength range	0.25 to 4.0 μm	Spectral irradiances computed at 20 cm^{-1} spectral resolution and integrated by trapezoidal rule.
	Surface reflectance	0.1	At 555 nm, from MODIS (Vermote et al., 1997). Spectral dependence is obtained by linearly interpolating values between seven wavelengths (0.469 to 2.13) and set equal to zero outside this wavelength range.
	Time	Diurnally averaged	Calculations carried out for solar zenith angles in steps of 3 degrees and weighted average is taken for one diurnal cycle.

February 2004 at 19.3° N latitude and 80.6° E longitude for higher altitudes. Though the SAGE profile is somewhat separated both in time as well as in location, it is a more realistic choice than using a model aerosol profile. The aerosol extinction profiles are scaled such that the integration of the complete profile equals to average AOD for that day. ARF computations are made for the measured as well as for 'standard' aerosol extinction profiles. Standard extinction profiles are those when actual measured information on aerosol vertical distribution is not available, but are calculated from visibility and AOD data (Ricchiazzi et al., 1998). Here, visibility is defined as V=3.912/α_g, where α_g is extinction coefficient (in km^{-1}) at ground level. Figure 6 shows the standard and observed extinction profiles for 17 February. Apart from extinction profile, one needs to know vertical profiles of single scattering albedo (SSA), and asymmetry parameter (AP) for calculating ARF. Spectral dependence of extinction-coefficient, SSA and AP and vertical profiles of SSA and AP are obtained from aerosol models (i) Continental Average (ii) Continental Clean (iii) Continental Polluted (iv) Desert and (v) Urban, by varying them independently for the boundary layer, free troposphere and stratosphere. Full description of these models is available in d'Almeida et al. (1991) and Hess et al. (1998). The aerosol types considered for the boundary layer are Continental Average, Continental Polluted, Urban and Desert. Aerosol types used for the free tropospheric region are Continental Average and Continental Clean and for the stratosphere, Continental Clean and Sulphate aerosols are used. These combinations resulted in 16 vertical distributions of single scattering albedo and asymmetry parameter and depending on the aerosol model used, radiative forcing values at the top of the atmosphere (TOA) ranges from +7 to $-1\,W/m^2$. Considering the geography of the measurement location (inland continental), the most suitable combination is found to be the "Continental Average" aerosol type for boundary layer, "Continental Clean" and "Sulphate" for the free troposphere and stratosphere regions respectively. Surface level SSA obtained at Shaadh Nagar from other independent measurements during the same period was about 0.87 at 525 nm (Ganguly et al., 2005) which is close to the SSA value of 0.85 prescribed for the "Continental Average" aerosol type. The ARF estimates for this combination of models for a standard extinction profile and the measured extinction profile on 17 February are compared in Fig. 7. While the surface level ARF is comparable for both the cases, the difference between the values increases with increasing

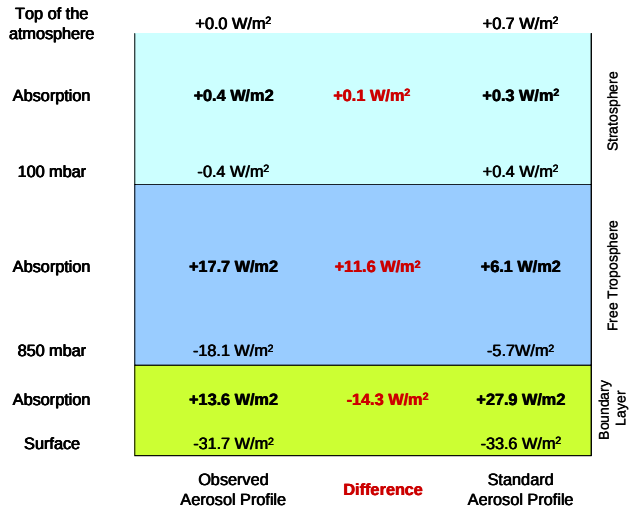

Fig. 7. Clear sky aerosol radiative forcing in the short wave region (0.25 to 4 μm) calculated for the profiles shown in Fig. 6 while the integrated column AOD and aerosol optical properties are kept same. Large differences are seen in the forcing values at higher altitude and at the top of the atmosphere. Values in regular font are aerosol radiative forcing at given altitude and values in bold font are atmospheric absorption due to aerosols.

altitude. For the standard aerosol profile, the atmospheric absorption due to aerosol within the boundary layer and in the free troposphere are +27.9 and +6.1 W/m^2, while the corresponding values obtained for the measured profile are +13.6 and +17.7 W/m^2, respectively. The free tropospheric absorption due to aerosol is underestimated in case of the standard aerosol profile. Atmospheric absorption is however a very sensitive parameter in climate change studies as it contributes to the heating rate and stability of atmosphere, which are important in atmospheric dynamics and cloud formation process. ARF estimates are also prone to large uncertainty due to uncertainty in prescribing the aerosol type, surface reflectance, etc. In this work we demonstrate that apart from these uncertainties knowledge on the vertical distribution of aerosols is also equally important to make a realistic estimate on atmospheric absorption due to aerosol. The difference in ARF values could be much larger in case of cloudy sky, which will be attempted in future studies.

5 Conclusion

For the first time feasibility of using a commercial lidar of MPL type on a small aircraft is established for the study of boundary layer height and aerosol vertical profile over urban locations. The study made over Hyderabad, an urban location in the central India proves the possibility of making low cost airborne lidar observations elsewhere. It is found that airborne lidar observation has a distinct advantage over ground based observations, particularly over heavily polluted locations, because of its capability to detect free tropospheric aerosols more accurately. Three different inversion algorithms suitable for analysing the airborne and space-borne lidar data viz. Palm et al. (2002), Stephens et al. (2001) and Klett (1985) are used and compared. No bias is found among three algorithms in retrieving the aerosol extinction coefficient from the lidar data. Lidar ratio estimated by constraining the extinction profile with independently measured column AOD is sensitive to the uncertainty in the aerosol backscattering coefficient at reference altitude. Error in the derived extinction profile can be reduced to a great extent if simultaneous measurements of scattering coefficient and/or optical depth of the free troposphere can be made onboard.

Detailed ARF computations are made using both the observed aerosol extinction profiles as well as for standard model extinction profile. It is shown that though both the profiles are normalized for the same column AOD and uses the same aerosol optical properties, the differences in the vertical distribution of aerosol yield very different results for the vertical distribution of ARF. Though the ARF values at the surface are comparable, appreciable differences are seen within the atmosphere at different altitude levels. In one example case, it is shown that for the same aerosol optical depth, standard aerosol extinction profile underestimates the free tropospheric aerosol absorption by 11.6 W/m^2 and overestimates the boundary layer absorption by 14.3 W/m^2 compared to that for the observed extinction profile.

Acknowledgements. The experiment was funded under the ISRO-Geosphere Biosphere Program. Authors would like to thank the National Remote Sensing Agency, Hyderabad for providing the necessary infrastructure and facilities to carry out the aircraft experiments, and their colleague J. T. Vinchhi for his technical assistance. Necessary SAGE-II aerosol data are obtained from http://www-sage2.larc.nasa.gov/ and MODIS surface reflectance data is obtained from http://edcdaac.usgs.gov/. Authors also thank the anonymous reviewers for their valuable comments and suggestions.

Topical Editor F. D'Andrea thanks two referees for their help in evaluating this paper.

References

Ackerman, M., Lippens, C., Brogniez, C., et al.: European validation of SAGE II aerosol profiles, J. Geophys. Res., 94(D6), 8399–8411, doi:10.1029/89JD00242, 1989.

Albrecht, B. A.: Aerosols, cloud microphysics, and fractional cloudiness, Science, 245, 1227–1230, 1989.

Campbell, J. R., Hlavka, D. L., Welton, E. J., Flynn, C. J., Turner, D. D., Spinhirne, J. D., Scott III, V. S., and Hwang, I. H.: Full-time, eye-safe cloud and aerosol lidar observation at atmospheric radiation measurement program sites: Instruments and data processing, J. Atmos. Oceanic Tech., 19, 431–442, 2002

d'Almeida, G. A., Koepke, P., and Shettle, E. P.: Atmospheric Aerosols: Global Climatology and Radiative Characteristics, A. Deepak Publishing, Hampton, Virginia, USA, 561 pp, 1991.

Devara, P. C. S., Raj, P. E., and Pandithurai, G.: Aerosol-profile measurements in the lower troposphere with four-wavelength bistatic argon-ion lidar, Appl. Opt. 34(21), 4416–4425, 1995.

Fernald, F. G., Herman, B. M., and Reagan, J. A.: Determination of aerosol height distributions by Lidar, J. Appl. Meteorol., 11, 482–490, 1972.

Flamant C., Pelon, J., Chazette, P., Trouillet, V., Quinn, P. K., Frouin, R., Bruneau, D., Leon, J.-F., Bates, T., Johnson, J., and Livingston, J.: Airborne lidar measurements of aerosol spatial distribution and optical properties over the Atlantic Ocean during an European pollution outbreak of ACE-2, Tellus, 52B, 662–677, 2000.

Gadhavi, H.: Experimental investigation of aerosol properties and modelling its impact on radiation budget, PhD Thesis, Gujarat University, Ahmedabad, India, 138 pp, 2005

Ganguly, D., Gadhavi, H., Jayaraman, A., Rajesh, T. A., and Misra, A.: Single scattering albedo of aerosols over the central India: Implications for the regional aerosol radiative forcing, Geophys. Res. Lett., 32, L18803, doi:10.1029/2005GL023903, 2005.

Hart, W. D., Spinhirne, J. D., Palm, S. P., and Hlavka, D. L.: Height distribution between cloud and aerosol layers from the GLAS spaceborne lidar in the Indian Ocean region, Geophys. Res. Lett., 32, L22S06, doi:10.1029/2005GL023671, 2005.

Haywood, J. and Boucher, O.: Estimates of the direct and indirect radiative forcing due to tropospheric aerosols: A review, Rev. Geophys., 38(4), 513–543, doi:10.1029/1999RG000078, 2000.

Hess, M., Koepke, P., and Schult, I.: Optical properties of aerosols and clouds: The software package OPAC, Bull. Am. Meteorol. Soc., 79, 831–844, 1998.

IPCC: Climate Change 2001: The Scientific Basis, Contribution of Working Group I to the Third Assessment Report of the Intergovernmental Panel on Climate Change, edited by: Houghton, J. T., Ding, Y., Griggs, D. J., et al., Cambridge University Press, New York, 881 pp, 2001.

Jayaraman, A., Subbaraya, B. H., and Acharya, Y. B.: The vertical distribution of aerosol concentration and their size distribution function over the tropics and their role in radiation transfer, Physica Scripta, 36, 358–361, 1987.

Jayaraman, A. and Subbaraya, B. H.: In situ measurements of aerosol extinction profiles and their spectral dependencies at tropospheric levels, Tellus, 45B, 473–478, 1993.

Jayaraman, A., Ramachandran, S., Acharya, Y. B., and Subbaraya, B. H.: Pinatubo volcanic aerosol layer decay observed at Ahmedabad (23 N) India using Nd:YAG backscatter lidar, J. Geophys. Res., 100, 23 209–23 214, 1995.

Kaestner, M.: Lidar inversion with variable backscatter/extinction ratios: comment, Appl. Opt., 25(6), 833–835, 1986.

Kaufman, Y. J., Koren, I., Remer, L. A., Rosenfeld, D., and Rudich, Y.: The effect of smoke, dust and pollution aerosol on shallow cloud development over the Atlantic Ocean, Proc. Nation. Acad. Sci. (USA), 102(32), 11 207–11 212, doi:10.1073/pnas.0505191102, 2005.

Kent, G. S., Trpte, C. R., and Lucker, P. L.: Long-term Stratospheric Aerosol and Gas Experiment I and II measurements of upper tropospheric aerosol extinction, J. Geophys. Res., 103, 28 863–28 874, 1998.

Klett, J. D.: Stable analytical inversion solution for processing lidar returns, Appl. Opt., 20(2), 211–221, 1981.

Klett, J. D.: Lidar inversion with variable backscatter/extinction ratios, Appl. Opt., 24(11), 1638–1643, 1985.

McClatchey, R. A., Fenn, R. W., Selby, J. E. A., Volz, F. E., and Garing, J. S.: Optical properties of the atmosphere, 3rd ed. AFCRL Environ. Res. Papers No. 411, 108 pp, 1972.

McGill, M. J., Hlavka, D. L., Hart, W. D., Welton, E. J., and Campbell, J. R.: Airborne lidar measurements of aerosol optical properties during SAFARI-2000, J. Geophys. Res., 108(D13), 8493, doi:10.1029/2002JD002370, 2003.

Palm, S. P., Hart, W., Hlavka, D., et al.: GLAS atmospheric data products, Algorithm Theor. Basis. Doc. ATBD-GLAS-01, version 4.2, Earth Obs. Syst. Proj. Off., Greenbelt, Md. (Available at http://eospso.gsfc.nasa.gov/eos_homepage/for_scientists/atbd/), 2002.

Parameswaran, K., Rajan, R., Vijayakumar, G., Rajeev, K., Moorthy, K. K., Nair, P. R., and Satheesh, S. K.: Seasonal and long term variations of aerosol content in the atmospheric mixing region at a tropical station on the Arabian sea-coast, J. Atmos. Solar-Terrestrial Phys., 60(1), 17–25, 1998.

Pelon, J., Flamant, C., Chazette, P., Leon, J.-F., Tanré, D., Sicard, M., and Satheesh, S. K.: Characterization of aerosol spatial distribution and optical properties over the Indian Ocean from airborne LIDAR and radiometry during INDOEX'99, J. Geophys. Res., 107(D19), 8029, doi:10.1029/2001JD000402, 2002.

Pincus, R. and Baker, M.: Precipitation, solar absorption, and albedo susceptibility in marine boundary layer clouds, Nature, 372, 250–252, 1994.

Ramachandran, S. and Jayaraman, A.: Balloon-borne study of the upper tropospheric and stratospheric aerosols over a tropical station in India, Tellus, 55(3)B, 820–836, 2003.

Ramanathan, V., Chung, C., Kim, D., et al.: Atmospheric brown clouds: Impacts on south Asian climate and hydrological cycle, Proc. Nation. Acad. Sci. (USA), doi:10.1073/pnas.0500656102, 2005.

Ramanathan, V., Crutzen, P. J., Lelieveld, J., et al.: Indian Ocean Experiment: An integrated analysis of the climate forcing and effects of the great Indo-Asian haze, J. Geophysic. Res., 106(22), 28 371–28 398, doi:10.1029/2001JD900133, 2001.

Ricchiazzi, P., Yang, S., Gautier, C., and Sowle, D.: SBDART: A research and teaching software tool for plane-parallel radiative transfer in the Earth's atmosphere, Bull. Am. Meteorol. Soc., 79(10), 2101–2114, 1998.

Rodger, C.: Retrieval of atmospheric temperature and composition from remote measurements of thermal radiation, Rev. Geophys., 14, 609–624, 1976.

Rodger, C.: Characterization and error analysis of profiles retrieved from remote sounding measurements, J. Geophys. Res., 95, 5587–5595, 1990.

Rodger, C.: Inverse methods for atmospheric sounding: Theory and Practice, World Scientific, 2, 238, 2000.

Spinhirne, J. D., Palm, S. P., Hart, W. D., Hlavka, D. L., and Welton, E. J.: Cloud and aerosol measurements from GLAS: Overview and initial results, Geophys. Res. Lett., 32, L22S03, doi:10.1029/2005GL023507, 2005.

Spinhirne, J.D.: Micro Pulse Lidar, IEEE Trans. Geosci. Remote Sens., 31, 48–55, 1993.

Stephens, G. L., Engelen, R. J., Vaughan, M., and Anderson, T. L.: Toward retrieving properties of the tenuous atmosphere using space-based lidar measurements, J. Geophys. Res., 106, 28 143–28 157, 2001.

Stunder, B.: NCEP Model Output – FNL Archive Data, References 134, National Climate Data Center, NOAA – Air Resources Laboratory, USA, 1997.

Twomey, S.: Pollution and the planetary albedo, Atmos. Environ., 8, 1251–1256, 1974.

Vermote, E. F., El Saleous, N. Z., Justice, C. O., Kaufman, Y. J., Privette, J., Remer, L. C., and Tanré, D.: Atmospheric correction of visible to middle infrared EOS-MODIS data over land surface, background, operational algorithm and validation, J. Geophys. Res., 102(14), 17 131–17 142, doi:10.1029/97JD00201, 1997.